Magnetically-oriented type I collagen-SiO2@Fe3O4 rods composite hydrogels tuning skin cell growth

Yupeng Shi, Yanling Li, Thibaud Coradin

Magnetically-oriented type I collagen-SiO_2@Fe_3O_4 rods composite hydrogels tuning skin cell growth

Yupeng Shi,[a,c] Yanling Li,[b] Thibaud Coradin*[a]

[a]*Sorbonne Université, CNRS, Laboratoire de Chimie de la Matière Condensée de Paris, 75005 Paris, France*

[b]*Sorbonne Université, CNRS, Institut Parisien de Chimie Moléculaire, 75005 Paris, France*

[c] *Present address: Department of MRI, The First Affiliated Hospital of Zhengzhou University, Zhengzhou 450052, China*

*corresponding author: Thibaud Coradin; e-mail: thibaud.coradin@sorbonne-universite.fr

Abstract

Conferring orientational order to biological hydrogels constitutes a fruitful strategy for the guided growth of cells. The ability of anisotropic magnetic particles to align along an external magnetic field appears as a particularly, yet poorly explored, strategy to achieve such an orientation in 3D. For this purpose, silica rods coated with magnetite nanoparticles were prepared. When dispersed in a collagen type I solutions, they could be aligned along the magnetic field generated by two plate magnets within five minutes, such an alignment being preserved during hydrogel formation. Both magnetic and rheological measurements evidenced that different structures could be obtained in the absence of the magnetic field and when it was applied parallel or perpendicular to the hydrogel surface. These variations in rods organization also impacted the growth of 2D cultures of Normal Human Dermal Fibroblasts, which was attributed to the higher affinity of the cells for type I collagen compared to silica. These composites have a clear potential as biomaterials associating cell guidance and drug delivery.

Keywords: collagen; silica; magnetic particles; cell guidance

1. Introduction

The incorporation of magnetic particles within biological hydrogels has already been explored for many applications [1], including bioseparation [2], drug delivery [3] and tissue engineering or regeneration [4-6]. In most of these area, the magnetic composite hydrogels are first prepared and an external magnetic field is then applied, *in vitro* or *in vivo*, to take advantage of the magnetization, relaxativity and/or heating properties of the particles [7]. A few studies also pointed out that the beneficial effect of external magnetic fields on tissue regeneration could be enhanced if the scaffold incorporate magnetic particles [8,9].

Another approach to take advantage of the specific properties of magnetic particles is to use their ability to align along an external field to control the topography (2D) or structure (3D) of bioactive materials [10-12]. While this can be achieved with spherical particles [13,14], optimal orientation may be favored using highly anisotropic particles, *i.e.* rod- or wire-shaped objects [15,16]. Focusing on iron oxides, as the most popular magnetic particles used for medical applications, many protocols are available to obtain magnetic particles with high aspect ratio [17-19]. Another type of particles that would be particularly interesting to incorporate within composite hydrogels are those based on silica. While being generally recognized as biocompatible when incorporated within implant materials, they have the benefit over iron oxide to be easily prepared as porous systems allowing for the efficient loading and release of bioactive molecules [20-22].

Several approaches have been proposed to combine silica and iron oxide within a single anisotropic particle, including co-precipitation [23], silica condensation on pre-formed magnetic particles [24], or, conversely, grafting of magnetic particles on pre-

formed silica nanoparticles [25]. However, to the best of our knowledge, none of these were previously incorporated within hydrogels to design oriented hosts for cell culture.

Type I collagen, as the major protein in mammalian tissues, is widely used in tissue repair materials [26,27]. Collagen molecules can orient under a strong magnetic field (> 1 T) and form anisotropic hydrogels [28-31]. The conditions for optimal orientations were shown to critically depend on collagen concentration and fibrillogenesis conditions [32]. It was possible to correlate the direction of fibroblasts growth within such hydrogels with the magnetically-induced collagen fibril orientation [33]. Such a guided growth was due to both preferred cell migration along the oriented fibers and inhibited growth perpendicular to them [34] More recently, hyaluronic acid (HA) was added to the precursor collagen solution and used for the encapsulation of chondrocytes [35]. It was shown that the glycosaminoglycan had a negative impact on fiber orientation under the external magnetic field and that both HA and cells altered the mechanical properties of the hydrogels. Nevertheless, oriented matrices were less prone to cell-mediated contraction. Altogether, the use of strong magnetic fields to obtain structurally-oriented cell-guiding collagen scaffolds has a huge potential but faces important issues related to the high sensitivity of type I collagen fibrillogenesis to physico-chemical conditions. In parallel, the possibility to confer orientational order to the collagen network by an indirect effect through the incorporation of magnetically-responsive systems has been studied. For instance, biofunctionalized magnetic beads as well as nanoparticles could be used to orient collagen networks under much weaker fields (< 10 mT), with a beneficial impact on the growth of neural and osteoblastic cells [13,36,37].

Whereas a few studies have demonstrated the ability of (nano)rods to improve the mechanical stability of collagen hydrogels, none of them used magnetic particles to control the material orientation [38,39]. In addition to the aforementioned advantages of silica-based particles in terms of biocompatibility and drug delivery, their combination

with collagen has already been demonstrated useful for bone and skin repair [40,41], which may benefit from controlled fiber orientation [37], and opening perpective in other tissue engineering applications such as nerve regeneration [36]. However, silica being diamagnetic, it may orient only under a strong magnetic field. On this basis, we have prepared here $SiO_2@Fe_3O_4$ anisotropic particles by direct formation of iron oxide on silica rods and incorporated them within type I collagen hydrogels. Conditions for rods alignment in the collagen solution under an external magnetic field were identified. From this, composites with particles aligned parallel or perpendicular to the gel surface could be obtained. Magnetic and rheological properties of the hydrogels were shown to vary with rods orientation. Furthermore, the growth of Normal Human Dermal Fibroblasts (NHDFs) showed a high dependence on the composite organization.

2. Experimental Section

2.1. Synthesis of $SiO_2@Fe_3O_4$ rods

The rod-like silica particles having lengths of *ca*. 3 μm and diameters of about 300 nm were synthesized from tetraethoxysilane and ammonia in the presence of polyvinylpyrrolidone, as reported by Kuijk et al. [42]. A solution of 30 g of PVP in 300 mL of n-pentanol was sonicated for 3 hours. Then 30 mL absolute ethanol, 8.4 mL ultrapure water and 2 mL of an aqueous 0.18 M sodium citrate dihydrate solution were added sequentially. After a short hand shaking of the flask, 6.75 mL of ammonia was added, the flask hand-shaken again and 3 mL of TEOS added. After shaking again, the flask was placed at 30°C in a water bath and left to react for 24 h. After this time, the reaction mixture was centrifuged at 2000 *g* for 20 min, the supernatant was removed and the remaining particles redispersed in ethanol. This centrifugation step was repeated two times with ethanol and two times with water at 1000 *g* for 15 minutes, and finally again with ethanol, one time at 1000 *g* and two times at 500 *g*.

$SiO_2@Fe_3O_4$ rods were prepared by high temperature thermal decomposition of iron-tris(acetylacetonate) in tetraethyleneglycol (TEG) in presence of silica rods by adaptation of the protocol of Qu et al. [43]. A dispersion of 100 mg of silica nanorods in 1 mL of water was sonicated for 30 min. Then 0.177 g (0.5 mmol) of $Fe(acac)_3$ and 10 g of TEG were added and the mixture heated to 110 °C under vacuum for 1 h and two additional hours to 200 °C under a nitrogen flow. The system was then refluxed at 300 °C for 1 h before being cooled down to room temperature. As the final products also include a small fraction of unbound iron oxide nanocrystals, acetone was added to the synthesis solution, and an external magnetic field was applied at the bottom of the vial to precipitate the rods. The supernatant that contained free nanocrystals was discarded. The process was repeated five times, and the final product was dried under vacuum.

2.2. Preparation of collagen-$SiO_2@Fe_3O_4$ composites

Composites were prepared by mixing a 10 $mg.mL^{-1}$ type I collagen (from rat tails) suspension in 17 mM acetic acid solution with a 10 X phosphate buffer saline (PBS) solution containing the suitable amount of $SiO_2@Fe_3O_4$ rods to reach a final pH of 7.0 and a final concentration of silica rods of 30 $mg.mL^{-1}$ [35]. Resulting sols were quickly dispatched into a shaped mold and incubated at 37ºC to trigger gel formation. Magnetic orientation was achieved using a home-made set up using two plate magnets (Nd 70 x 50 x5 mm Ni-Cu-Ni N45 purchased from Superaimants) with controlled inter-distance [44]. Except when noted, the collagen-$SiO_2@Fe_3O_4$ solutions were prepared as described above, placed in the set-up and left to orient for 5 minutes before being placed in the incubator.

2.3 Material characterization

X-Ray Diffraction (XRD) pattern of the SiO_2@Fe_3O_4 powder was recorded in the 10-70° 2θ range using a Philips PW131 diffractometer using the Cu K_α radiation. X-Ray Photoelectron Spectroscopy (XPS) was performed on a SPECS GmbH Phoibos 100 spectrometer (Mg K_α X-ray source). Spectrum of the SiO_2@Fe_3O_4 powder was recorded in the Fe 2p region with a 10 eV pass energy. A takeoff angle of 90° from the surface was employed. The spectrum was analyzed using the Casa XPS v.2.3.13 Software (Casa software Ltd. U.K.)

Direct current magnetization was measured on a Quantum Design MPMS-XL magnetometer equipped with a 7 T dc magnet. The hysteresis curves were measured at 2 K and 200 K. The zero-field cooled–field cooled (ZFC–FC) measurements were performed at 100 Oe in the 2-250 K temperature range at a $2K.min^{-1}$ rate. A water insoluble polycarbonate capsule was selected as a sample holder. The SiO_2@Fe_3O_4 sample was introduced as a powder while the composite gels were formed directly within the capsule using the procedure described above. Both temperature and field variable data were corrected from the diamagnetic contribution of the sample holder and, when relevant, of collagen.

Rheological studies under shear oscillation were performed on wet composites in a disc form using a Bohlin Gemini rheometer (Malvern) equipped with a flat acrylic 40 mm diameter geometry. Mechanical spectra were recorded at 37 °C with a 1% applied strain. Gap between base and geometry was adjusted for each measurement to insure suitable contact with the hydrogel during shearing. Three samples of each hydrogel were tested.

For transmission electron microscopy (TEM) imaging, nanocomposites were fixed with 4% PFA in PBS and then in 2% osmium tetroxide in cacodylate/sucrose buffer (0.05 M/0.3 M, pH 7.4). After dehydration with ethanol, they were embedded in araldite. Thin araldite transverse sections (100-200 nm) were performed using a Ultracut

7 ultramicrotome (Reichert, France) and further stained using phosphotungstic acid. Imaging was performed with a Tecnai spirit G2 electron microscope operating at 120 kV.

2.4. Biological studies

Normal Human Dermal Fibroblasts (NHDF) were grown in complete cell culture medium (Dulbecco's Modified Eagle's Medium (DMEM) with GlutaMAX™, without phenol red supplement, with 10% fetal serum, 100 $U.mL^{-1}$ penicillin, 100 μg/mL streptomycin). Tissue culture flasks (75 cm^2) were kept at 37 °C in a 95% air: 5% CO_2 atmosphere. Before confluence, the cells were removed from flasks by treatment with 0.1% trypsin and 0.02% EDTA, rinsed and resuspended in the culture medium. NHDFs were seeded onto freshly-prepared nanocomposite discs (*i.e.* in 2D cultures) at a density of 5,000 $cells.cm^{-2}$. After 48 h of culture, cell activity was monitored by the Alamar Blue assay. All experiments were performed as triplicates.

For fluorescence microscopy, cells were treated with 4% PFA and 0.5 % Triton X-100 for 15 min. After rinsing, staining of actin with Alexa Fluor 488 phalloidin and nuclei with 4',6'-Diamidino-2-phenylindole (DAPI) solution was performed

3. Results .

Silica rods with dimensions of 245 ± 64 nm over 3.3 ± 0.8 μm were synthesized following the Kuijk protocol [42], and used as supports for the growth of iron oxide nanoparticles by a polyol route [43]. The iron content of the rods, as obtained by Inductively coupled plasma quadrupole mass spectrometry (ICP-QMS), was 9.6 wt%, corresponding to *ca.* 13 wt% Fe_3O_4. The successful coating of the surface of the silica rods by iron oxide nanoparticles can be clearly evidenced on the TEM images (**Fig. 1** and **Fig. S1** in Supplementary Data).

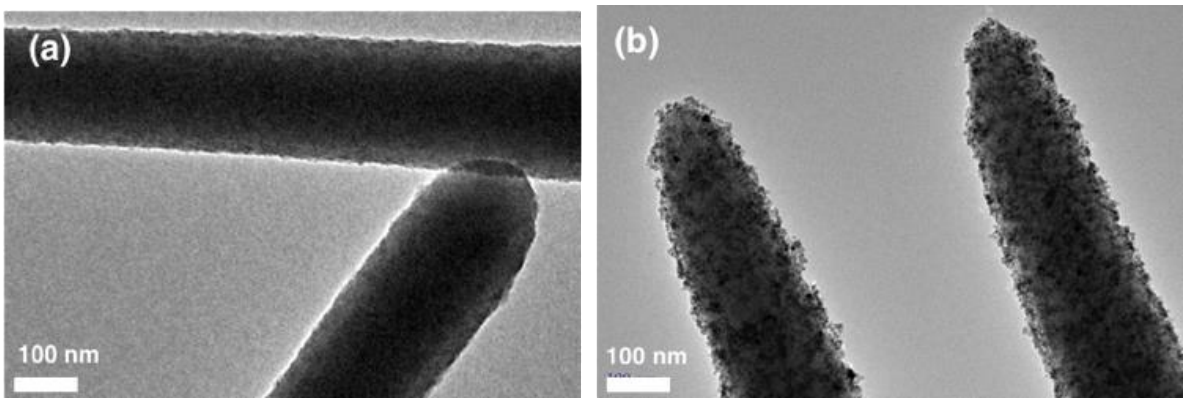

Fig. 1. TEM images of (a) bare and (b) iron oxide coated silica rods

A high density of nanoparticles having an average diameter of *ca.* 10 nm forms a thin layer which is almost uniformly distributed over the rods surface. This size range was in good agreement with that obtained for iron oxide nanoparticles prepared by the same method but in the absence of silica nanorods (**Fig. S2**). No separate magnetite nanoparticles were observed near the silica or in any other sample area after the washing procedure. To examine the stability of the magnetite on the silica surface, a small vial containing a dispersion of as-prepared $SiO_2@Fe_3O_4$ was immersed in a 40 kHz ultrasonic bath for several different time intervals. No observable change was observed for the samples after continuous ultrasonic treatment (**Fig. S3**), suggesting strong interactions between deposited nanoparticles and the silica surface.

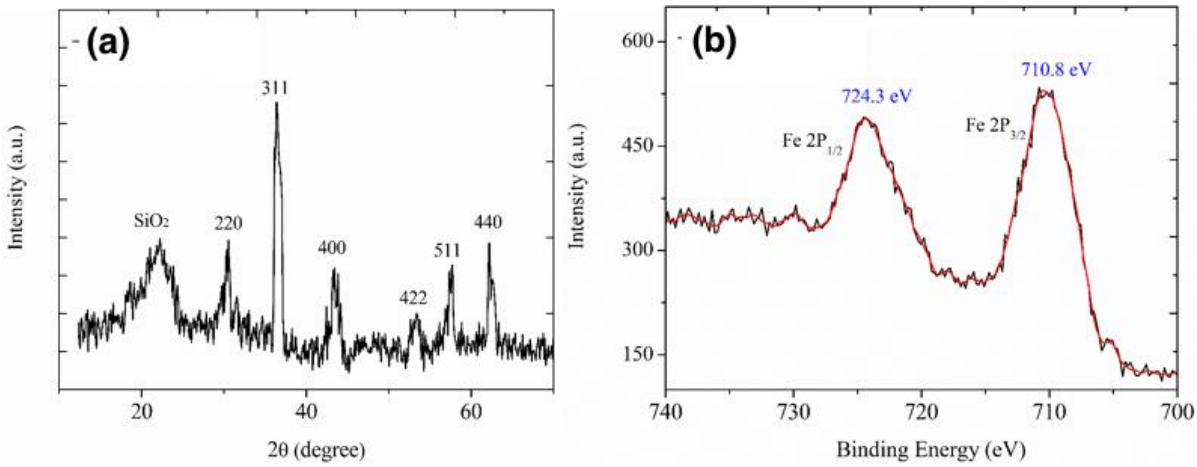

Fig. 2.(a) XRD pattern and (b) XPS spectra at the Fe_{2p} threshold of SiO_2 @Fe_3O_4 rods.

XRD analysis confirmed that the nanocrystals on the silica surface consisted of magnetite (**Fig. 2(a)**). The as-prepared materials were studied by XPS (**Fig. 2(b)**). The two photoelectron peaks at 710.6 and 724.1 eV are very close to those previously reported for core-level Fe_{2p} lines in magnetite [45], confirming the phase of the iron oxide nanoparticles on silica surface. As a first insight into the magnetic properties of the modified nanorods, we observed that applying a magnet at the proximity of a SiO_2@Fe_3O_4 aqueous suspension allows for its fast and efficient attraction to the glassware wall (**Fig. S4**).

The magnetic properties of as-synthesized SiO_2@Fe_3O_4 were then studied using a SQUID magnetometer. **Fig. 3(a)** shows the magnetization of the SiO_2@Fe_3O_4 powder as a function of applied field, recorded at 2 K and 200 K. An open hysteresis loop is observed at 2 K with a coercive field H_c = 729 Oe. The hysteresis curve is substantially saturated at the highest applied field (> 0.6 T). However, at 200 K, the hysteresis loop becomes a straight line and the coercive field is almost zero. **Fig. 3(b)** shows the zero-field-cooled (ZFC) and field-cooled (FC) magnetization of a powder sample of SiO_2@Fe_3O_4. The ZFC magnetization curve increases with temperature, reaching a

maximum at T = 74.3 K, which can be assumed, as a first approximation, to coincide with the blocking temperature T_B. The FC curve increases as the temperature decreases and never reaches saturation at low temperature, suggesting that interparticle interactions do not significantly affect the relaxation dynamics. The ZFC and FC curves start to diverge at a temperature far above the estimated T_B. This can be attributed to the relatively broad size and shape distributions of the samples.

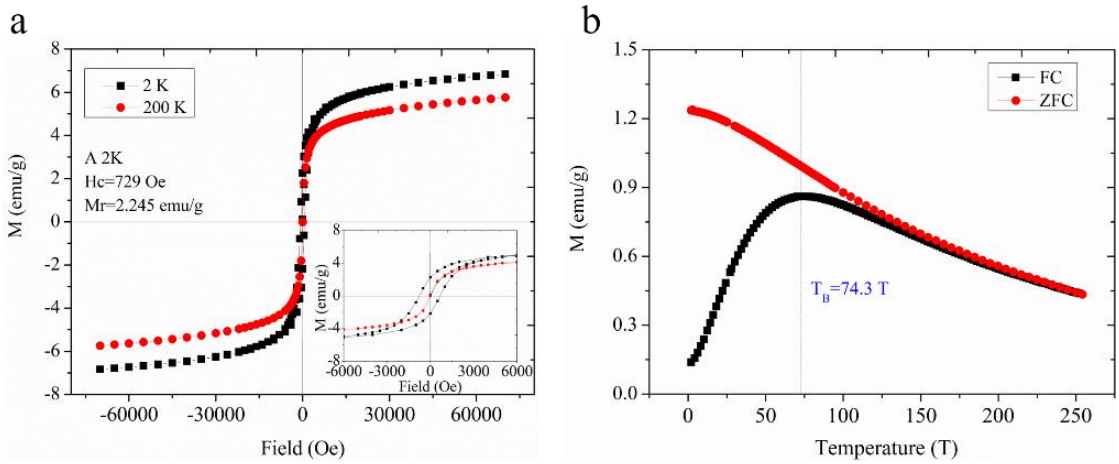

Fig. 3. (a) Magnetization curves at 2 K (dark) and 200 K (red) and (b) FC/ZFC curves at 100 Oe of SiO_2 @Fe_3O_4 rods powder.

The magnetic composite hydrogels were prepared by mixing magnetic rods with type I collagen solutions and inducing self-assembly by pH increase [39], first in the absence of external magnetic field. TEM images evidenced sections of the nanorods with various orientations, as previously reported for pure silica rods (**Fig. 4(a)**) [39]. The thin layer of magnetic nanoparticles coating the rods was also easily visualized (**Fig. 4(b)**). The background collagen network was difficult to observe, probably due to the high contrast of the iron oxide nanoparticles.

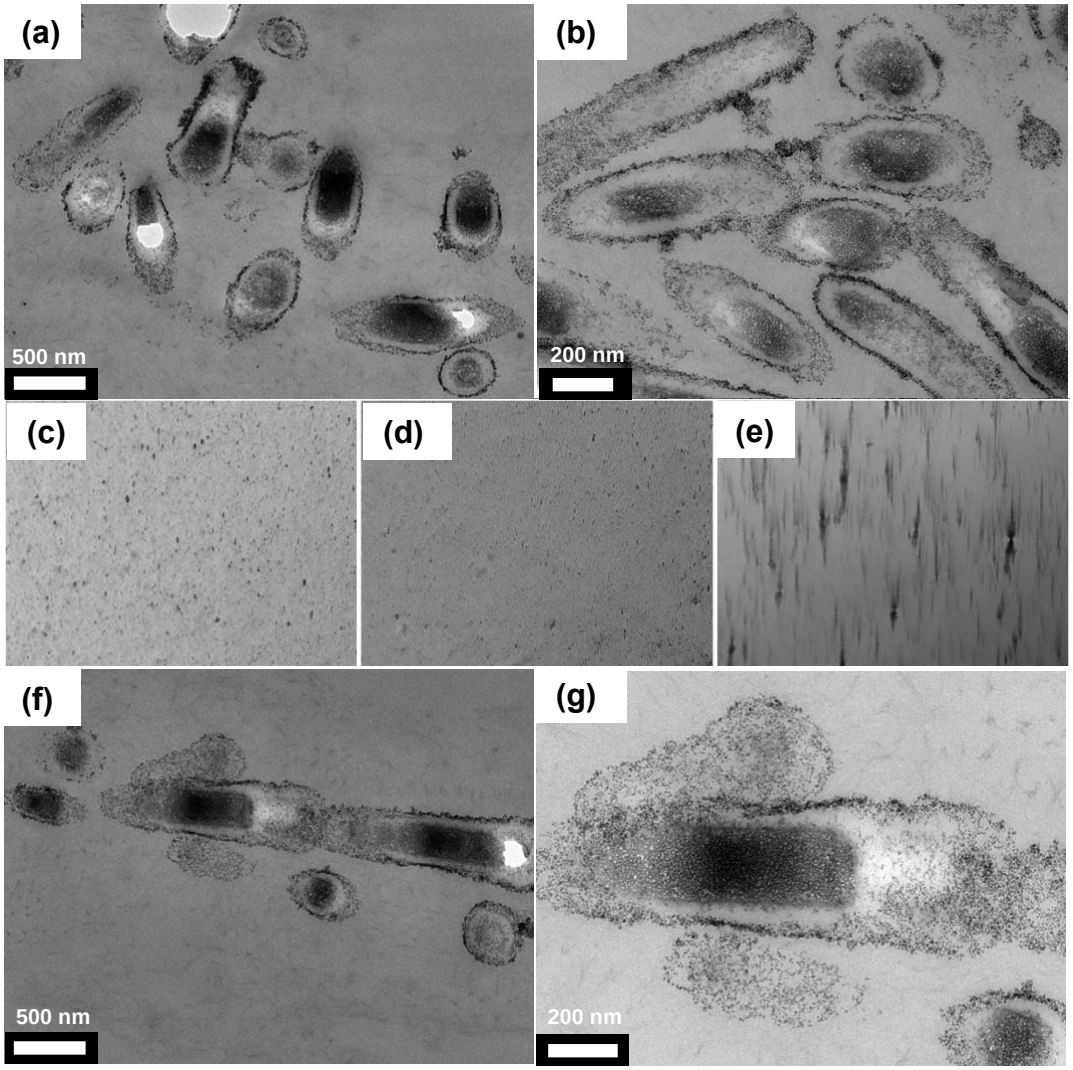

Fig. 4. (a)-(b) TEM images of non-oriented collagen-magnetic particles composites; (c-e) bright-field optical microscopy images of magnetic particles in the acidic collagen solutions after 0, 2 and 5 minutes to magnetic plates; (f)-(g) TEM images of oriented collagen-magnetic particles composites.

Indeed, once the collagen matrix is formed, the nanorods can no longer orient when an external magnetic field is applied. Such an orientation must therefore be achieved in the acidic collagen-nanoparticle mixture before inducing gelation. In preliminary experiments, a drop of the collagen solution at 10 $mg.mL^{-1}$ containing 30 $mg.mL^{-1}$ magnetic rods was deposited on a glass slide and placed between two plate magnets. The two plates were oriented with opposite poles (*i.e.* fields in same direction) facing each other. We conducted a study of the kinetics of the process under the

microscope and, as shown in **Fig. 4(c)-(e)**, it took only 5 minutes for the nanorods to be aligned. These conditions were then repeated for bulk hydrogels and the resulting composites were imaged by TEM. As seen on **Fig. 4(f)-(g)**, it seems that two nanorod orientations are favored, one parallel to the plane of the image, one perpendicular to it. Two rods well aligned along their main axis are also observed.

Subsequently, we prepared samples of magnetic hydrogel composites in three different configurations, (i)- no field, (ii)- field parallel to hydrogel surface, (iii)- field perpendicular to gel surface (**Fig. 5(a)**). These hydrogels were formed directly in the polymer capsule used for SQUID measurements, allowing to preserve their initial orientation when placed in the machine. Whereas composite hydrogels obtained without applied magnetic field or field applied parallel to the upper gel surface have almost identical magnetic behaviors, sample (iii) is clearly different: it presents a wider hysteresis at 2 K (**Fig. 5(b)**) and higher magnetizations in FC/ZFC curves (**Fig. 5(c)**) than the two other samples. This should be related to the relative direction of the magnetic field within the SQUID equipment compared to the favored orientation of the nanorods within the samples.

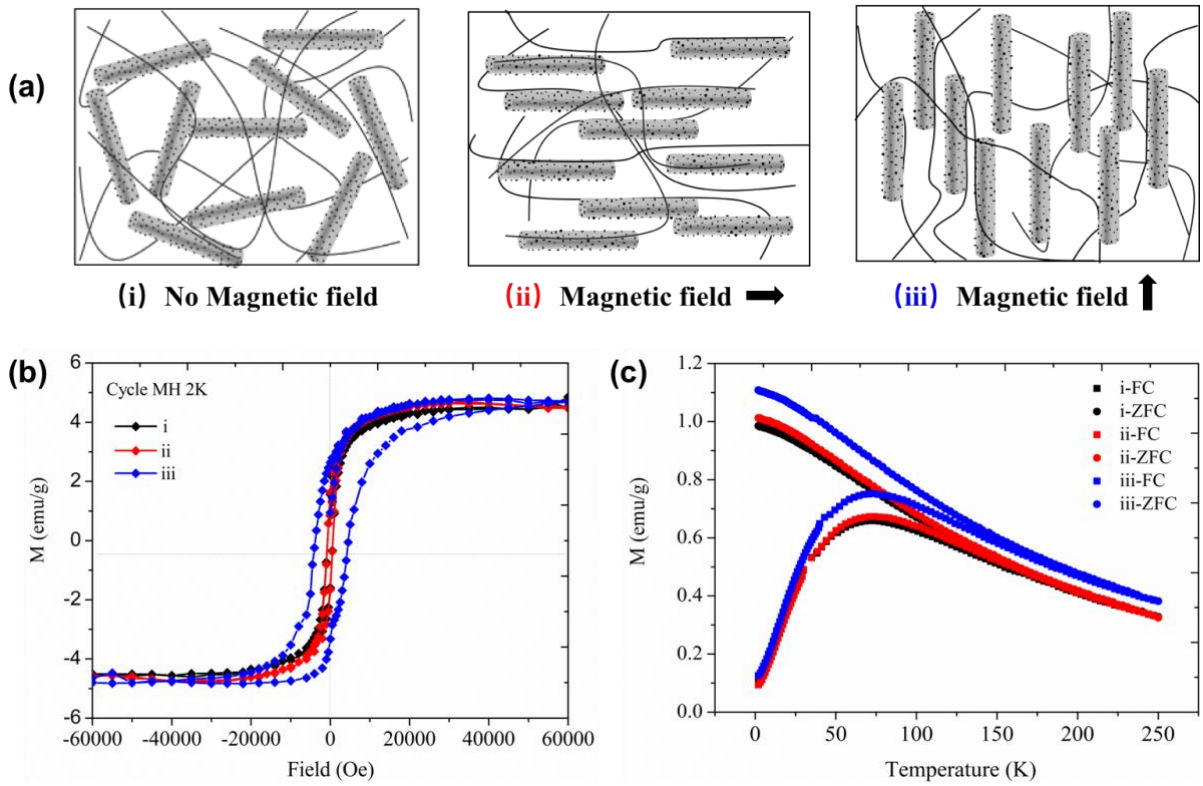

Fig. 5. (a) Schematic representation, (b) magnetization curves at 2 K and (c) FC-ZFC curves at 100 Oe for the un-oriented (i) and oriented (ii,iii) composite hydrogels. Magnetization is given per g of dry matter for direct comparison with rods alone.

In parallel, when the rheological properties under a shear stress parallel to the upper gel surface were measured, statistically smaller storage (*G'*) and loss (*G''*) values were found for sample (iii) (**Fig. 6(a)**) compared to the two other configurations. One possible explanation is that in the configuration of rheological measurements, the shear stress is applied parallel to the gel surface. Thus both methods are able to distinguish between vertically-oriented samples and horizontally or random composites. Although the effects are small, they at least indicate that the applied magnetic field had a measurable impact on the organization of the rods.

To check whether such structural modification could impact on cell behavior, Normal Human Dermal Fibroblasts (NHDFs) were seeded and cultured on the three

types of gel. Monitoring of cell activity after 48 h by the Alamar blue showed a significant increase of cell survival between un-oriented (i) and oriented (ii) and (iii) samples. The average value of cell activity was found higher for the perpendicularly-oriented system compared to parallel orientation, although the difference was not statistically significant (**Fig. 6(b)**).

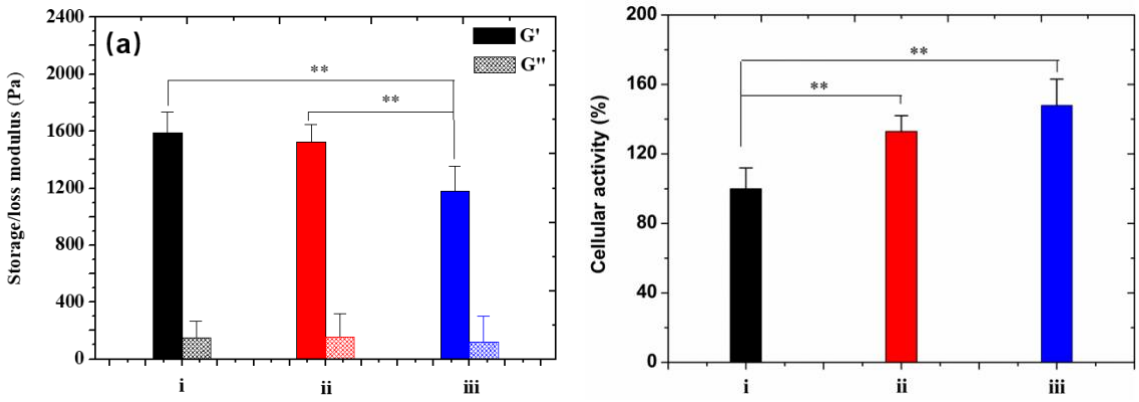

Fig. 6. Influence of rods orientation on (a) rheological properties of the composites and (b) cellular activity (%) after 48 h of NHDFs (un-oriented sample taken as the reference), with (i) un-oriented sample, (ii) sample prepared with magnetic field parallel to the surface and (iii) sample prepared with magnetic field perpendicular to the surface. Statistical significance was calculated by t-test analysis (* $p < 0.05$, ** $p < 0.01$).

The differences in cell growth between the two extreme cases (i) and (iii) were clearly evidenced by fluorescence microscopy (**Fig. 7**). Moreover, whereas most cells appear to have grown in an aligned manner on the whole surface of sample (ii), *i.e.* with rods parallel to the surface, they appear to be clustered in domains on sample (iii).

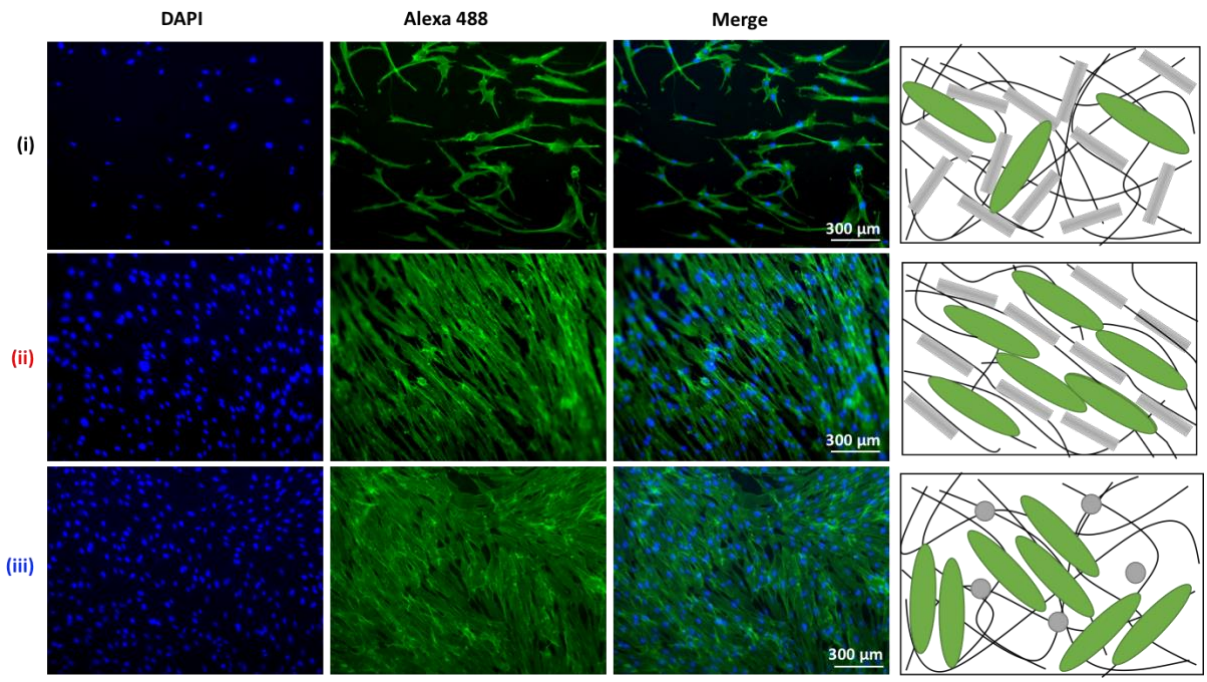

Fig. 7. Fluorescence microscopy images and schematic representation of NHDFs culture on composite hydrogels after 48 h. Nuclei were stained with DAPI and actin with Alexa Fluor 488 (magnification x10).

4. Discussion

The many benefits of high aspect ratio magnetic particles over their spherical equivalents are now well-recognized [46]. In the case of iron oxide, the templating approach is probably the most popular to prepare them as the shape of the final particle is not limited by the intrinsic constraints of their growth mechanism [47]. Here we used a simple method to prepare silica rods [42] and selected a recently-described protocol to firmly attach the iron oxide nanoparticles on their surface [43]. XRD and XPS analyses evidenced that the magnetite phase was formed and the magnetization at saturation at 2 K of *ca.* 6 emu per g of SiO_2@Fe_3O_4 powder containing *ca.* 13 wt% Fe_3O_4, *i.e.* 45 emu per g of magnetite, is also consistent with the literature [48].

In the absence of external magnetic field, these rods can be mixed with an acidic collagen solution and incubated to form a composite hydrogel. TEM suggests a random orientation of the rods. As a matter of fact, the measured *G'* value is similar to the one

previously reported for composites of same silica and collagen concentrations but with bare rods (*ca.* 1700 Pa), which is higher than that of the collagen hydrogel alone (*ca.* 1400 Pa) [39], suggesting that the presence of iron oxide particles has no impact on the composite hydrogel structure. The magnetization at saturation at 2K is *ca.* 4.5 emu per g of dry matter. Compared with the magnetization of silica-iron oxide powder alone (*ca.* 6 emu per g), this value is consistent with its 10 collagen:30 $SiO_2@Fe_3O_4$ weight ratio and suggests no significant loss of iron oxide during the hydrogel synthesis.

When placed between two parallel plate magnets (field 50-80 mT) [44], it was possible to achieve a significant alignment of the rods in the collagen solution within 5 minutes, which may be favored by the shear thinning behavior of such solutions [49]. Importantly, TEM images suggest that this alignment is preserved during the few minutes required for hydrogel formation. Such a preservation of rods orientation may be due to the high viscosity of the collagen solution, with a reported zero-shear viscosity > 500 Pa.s [43], to be compared with *ca.* 0.2 Pa.s for a 1 wt% alginate solution [50].

In terms of rheological properties, rods orientation parallel to the gel surface did not significantly modify the *G'* value compared to the un-oriented ones whereas a clear decrease in this value was observed for rods oriented perpendicular to the surface. Accordingly, the magnetic properties of un-oriented and parallel samples were similar whereas the perpendicular sample had significantly larger hysteresis width at 2K and higher magnetization values on the ZFC-FC curves, with no variation in T_B. On the one hand, it suggests that in the un-oriented hydrogel, rods are preferentially standing parallel to the surface, which may be due to their partial settling in the course of gel formation, as expected for micron size objects. Importantly, such a similarity between the un-oriented and parallel sample also supports the assumption that collagen fibers are not oriented by the magnetic field, due to its low intensity. On the other hand, the

variation in magnetic properties may reflect the intrinsic magnetic anisotropy of iron oxide nanoparticles and would indicate that particles deposited on the rods surface are not randomly oriented.

Ultimately, the NHDFs response to the hydrogels offers the most convincing evidence of the ability of the external magnetic field to control rods orientation. In the absence of this field, cells grow to a moderate extent while growth is much marked for the two other samples, with different cell organizations as a function of rods orientation. These observations can be interpreted in light of the previous studies performed on randomly-oriented collagen-silica rods composites [39]. They show that the silica rods constitute unfavorable surfaces for NHDFs adhesion and proliferation, in contrast to collagen. Therefore, cells preferentially grow in collagen-rich area between the rods. In the un-oriented samples, these areas may be of limited size, allowing for local cell adhesion but not proliferation. When rods are oriented parallel to the surface, they may define channels that guide the cells growth in one direction. Finally, when rods are perpendicular to the surface, the collagen area are much larger and NHDF cells can proliferate until they come in contact with the extremity of the rods (**Fig. 7**).

5. Conclusions

Highly anisotropic silica-based particles were prepared, that could be easily oriented in a type I collagen solution by a weak (< 100 mT) magnetic field, this alignment being preserved within the formed hydrogel. The orientation has a significant but moderate impact on the rheological and magnetic properties of the resulting composite. In contrast, its influence on the growth of fibroblasts was much more marked, suggesting that silica rods alignment defines boundaries of domains where cell adhesion and proliferation is favoured. Considering the well-recognized potentialities of silica-based particles for

drug release, here-described composite hydrogels are highly promising biomaterials to combine cell guidance and controlled delivery of bioactive molecules.

Acknowledgements

This work was supported by a PhD grant from the China Scholarship Council. B. Haye (LCMCP) is thanked for performing ultrathin sections for TEM imaging, C. Hélary (LCMCP) for his help for cell culture experiments and Y. Journaux (IPCM) for his advice on magnetic measurements.

References

[1] Y. Li, G. Huang, X. Zhang, B. Li, Y. Chen, T. Lu, T. J. Lu, F. Xu. Magnetic Hydrogels and Their Potential Biomedical Applications. Adv. Funct. Mater., 23 (2013), pp. 660-672.

[2] C. Xu, K. Xu, H. Gu, X. Zhong, Z. Guo, R. Zheng, C. Zhang, B. Xu. Nitrilotriacetic Acid-Modified Magnetic Nanoparticles as a General Agent to Bind Histidine-Tagged Proteins. J. Am. Chem. Soc., 126 (2004), pp. 3392-3393.

[3] R. Sensenig, Y. Sapir, C. MacDonald, S. Cohen, B. Polyak. Magnetic nanoparticle-based approaches to locally target therapy and enhance tissue regeneration in vivo. Nanomedicine, 7 (2012), pp. 1425-42.

[4] L. Rödling, E.M. Volz, A. Raic, K. Brändle, M. Franzred, C. Lee-Thedieck. Magnetic Macroporous Hydrogels as a Novel Approach for Perfused Stem Cell Culture in 3D Scaffolds via Contactless Motion Control. Adv. Healthc. Mater., 7 (2018), e1701403.

[5] V. Du, N. Luciani, S. Richard, C. Gay, F. Mazuel, M. Reffay, P. Menasché, O. Agbulut, C. Wilhem. A 3D magnetic tissue stretcher for remote mechanical control of embryonic stem cell differentiation. Nature Comm., 8 (2017), 400.

[6] X. Guan, M. Avci-Adali, E. Alarçin, H. Cheng, S.S. Kashaf, Y. Li, A. Chawla, H.L. Jang, A. Khademhosseini, Development of hydrogels for regenerative engineering. Biotechnol. J., 12 (2017), 201600394.

[7] S. Gil, J. F. Mano. Magnetic composite biomaterials for tissue engineering. Biomater. Sci., 2 (2014), pp. 812-818.

[8] S. Panceri, A. Russo, M. Sartori, G. Giavaresi, M. Sandri, M. Fini, M.C. Maltarello, T. Shelyakova, A. Ortolani, A. Visani, V. Dediu, A. Tampieri, M. Marcacci. Modifying bone scaffold architecture in vivo with permanent magnets to facilitate fixation of magnetic scaffolds. Bone, 56 (2013), pp. 432-439.

[9] Y. Xia, J. Sun, L. Zhao, F. Zhang, X.-J. Liang, Y. Guo, M.D. Michael, M.A. Reynolds, N. Gu, H.H.K. Xu. Magnetic field and nano-scaffolds with stem cells to enhance bone regeneration. Biomaterials, 183 (2018) pp. 151-170.

[10] J. Kim, J.R. Staunton, K. Tanner. Independent Control of Topography for 3D Patterning of the ECM Microenvironment. Adv. Mater., 28 (2016) pp. 132-137.

[11] D. Yang, B. Lu, Y. Zhao, X. Jiang. Fabrication of Aligned Fibrous Arrays by Magnetic Electrospinning. Adv. Mater., 19 (2007), pp. 3702-3706.

[12] J.D. Kiang, J.H. Wen, J.C. del Alamo, A.J. Engler. Dynamic and reversible surface topography influences cell morphology. J. Biomed. Mater. Res. A., 101 (2013), pp. 2313-2321.

[13] C. Guo, L.J. Kaufman. Flow and magnetic field induced collagen alignment. Biomaterials, 28 (2007), pp. 1105-1114.

[14] A.B. Bonhomme-Espinosa, F. Campos, I.A. Rodriguez, V. Carriel, J.A. Marrins, A. Zubarev, J.D.G Duran, M.T. Lopez-Lopez. Effect of particle concentration on the microstructural and macromechanical properties of biocompatible magnetic hydrogels. Soft Matter, 13 (2017), pp. 2928-2941.

[15] A. Sharma, M.D. DiVito, D.E. Shore, A.D. Block, K. Pollock, P. Solheid, J.M. Feinberg, J. Modiano, C.H. Lam, A. Hubel, B.J.H. Stadler. Alignment of collagen matrices using magnetic nanowires and magnetic barcode readout using first order reversal curves (FORC), J. Magn. Magn. Mater., 459 (2018), pp. 176-181.

[16] M.M. Abrougui, M.T. Lopez-Lopez, J.D.G. Duran. Mechanical properties of magnetic gels containing rod-like composite particles. *Phil. Trans. R. Soc. A,* 377 (2019) 20180218.

[17] L. Suber, O. Imperatori, G. Ausanio, F. Fabbri, H. Hofmeister. Synthesis, morphology, and magnetic characterization of iron oxide nanowires and nanotubes. J. Phys. Chem. B, 109 (2005), pp. 7103-7109.

[18] Y.M Zhao, Y.-H. Li, R.Z. Ma, D.G. McCartney, Y.Q. Zhu. Growth and characterization of iron oxide nanorods/nanobelts prepared by a simple iron-water reaction. Small, 3 (2006), pp. 422-427.

[19] J. Mohapatra, A. Mitra, H. Tyagi, D. Bahadur, M. Aslam. Iron oxide nanorods as high-performance magnetic resonance imaging contrast agents. Nanoscale, 7 (2015), pp. 9174-9184.

[20] Z. Li, J.C. Barnes, A. Bosoy, J.F. Stoddart, J.I. Zink. Mesoporous silica nanoparticles in biomedical applications. Chem. Soc. Rev., 41 (2012) pp. 2590-25605.

[21] Y. Wang, Q. Zhao, N. Han, L. Bai, J. Li, J. Liu, E. Che, L. Hu, Q. Zhang, T. Jiang, S. Wang. Mesoporous silica nanoparticles in drug delivery and biomedical applications. Nanomedicine, 11 (2015), pp. 313-327.

[22] M. Vallet-Regi, M. Colilla, I. Izquierdo-Barba, M. Manzano. Mesoporous Silica Nanoparticles for Drug Delivery: Current Insights. Molecules, 23 (2018), E47.

[23] S.A. Corr, Y.K. Gun'ko, A.P. Douvalis, M. Venkatesan, R.D. Gunning, P.D. Nellist. From Nanocrystals to Nanorods: New Iron Oxide− Silica Nanocomposites From Metallorganic Precursors. J. Phys. Chem. C, 112 (2008) pp. 1008-1018.

[24] B.P. Burke, N. Baghdadi, A.E. Kownacka, S. Nigam, G.S. Clemente, M.M. Al-Yassiry, J. Domarkas, M. Lorch, M. Pickles, P. Gibbs, R. Tripier, C. Cawthorne, S.J. Archibald. Chelator free gallium-68 radiolabelling of silica coated iron oxide nanorods *via* surface interactions. Nanoscale, 7 (2015), pp. 14889-14869.

[25] S. Giri, B.G. Trewyn, M.P. Stellmaker, V. S. Lin. Stimuli-responsive controlled-release delivery system based on mesoporous silica nanorods capped with magnetic nanoparticles. Angew. Chem. Int. Ed. Eng., 44 (2005), pp. 5038-5044.

[26] R. Parenteau-Bareil, R. Gauvin, F. Berthod. Collagen-Based Biomaterials for Tissue Engineering Applications. Materials, 3 (2010), pp. 1863-1887.

[27] E.E. Antoine, P.P. Vlachos, M.N. Rylander. Review of collagen I hydrogels for bioengineered tissue microenvironments: characterization of mechanics, structure, and transport. Tissue Eng. Part B Rev., 20 (2014), pp. 683-696.

[28] J. Torbet, M-C. Ronzière. Magnetic alignment of collagen during self-assembly. Biochem. J., 219 (1984), pp. 1057-1059.

[29] N.S. Murthy. Liquid crystallinity in collagen solutions and magnetic orientation of collagen fibrils. Biopolymers, 23 (1984), pp. 1261-1267.

[30] J. Torbet, M. Malbouyres, N. Builles, V. Justin, O. Damour, A. Oldberg, F. Ruggiero, D. J. Hulmes. Orthogonal scaffold of magnetically aligned collagen lamellae for corneal stroma reconstruction. Biomaterials, 28 (2007), pp. 4268-4276.

[31] S. Chen, N. Hirota, M. Okuda, M. Takeguchi, H. Kobayashi, N. Hanagata, T. Ikoma. Microstructures and rheological properties of tilapia fish-scale collagen hydrogels with aligned fibrils fabricated under magnetic fields. Acta Biomater., 7 (2011) 644-652.

[32] S. Guido, R.T. Tranquillo, A methodology for the systematic and quantitative study of cell contact guidance in oriented collagen gels. J. Cell Sci., 105 (1993) 317-331.

[33] R.B. Dickinson, S. Guido, R.T. Tranquillo. Biased cell migration of fibroblasts exhibiting contact guidance in oriented collagen gels. Ann. Biomed. Eng., 22 (1994) 342-356.

[34] G.S. Shannon, T. Novak, C. Mousoulis, S.L. Voytik-Harbin, C.P. Neu. Temperature and concentration dependent fibrillogenesis for improved magnetic alignment of collagen gels. RSC Adv., 5 (2015) 2113-2121.

[35] T. Novak, S.L. Voytik-Harbin, C.P. Neu. Cell encapsulation in a magnetically aligned collagen–GAG copolymer microenvironment. Acta Biomater., 11 (2015) 274-282.

[36] M. Antman-Passig, O. Shefi, Remote Magnetic Orientation of 3D Collagen Hydrogels for Directed Neuronal Regeneration. Nano Lett., 16 (2016), pp. 2567-2573.

[37] A. Tampieri, M. Iafisco, M. Sandri, S. Panseri, C. Cunha, S. Sprio, E. Savini, M. Uhlarz, T. Herrmannsdörfer. Magnetic bioinspired hybrid nanostructured collagen-hydroxyapatite scaffolds supporting cell proliferation and tuning regenerative process. ACS Appl. Mater. Interfaces, 61 (2014) 15697-15707.

[38] M. Vedhanayagam, B.U. Nair, K.J. Sreeram. Collagen-ZnO Scaffolds for Wound Healing Applications: Role of Dendrimer Functionalization and Nanoparticle Morphology. ACS Appl. Bio. Mater., 2018, **1**, 1942-1958.

[39] Y. Shi, C. Hélary, T. Coradin. Exploring the cell–protein–mineral interfaces: Interplay of silica (nano)rods@collagen biocomposites with human dermal fibroblasts. Mater. Today Bio, 1 (2019) 100004.

[40] S. Heinemann, T. Coradin, M.F. Desimone. Bioinspired silica-collagen materials: applications and perspectives in the medical field, Biomater. Sci. 1 (2013) 688-702.

[41] A.M. Mebert, G.S. Alvarez, R. Peroni, C. Illoul, T. Coradin, M.F. Desimone. Collagen-silica nanocomposites as dermal dressings preventing infection in vivo. Mater. Sci. Eng. C, 93 (2018) 170-177.

[42] A. Kuijk, A. van Blaaderen, A. Imhof. Synthesis of monodisperse, rodlike silica colloids with tunable aspect ratio. J. Am. Chem. Soc., 133 (2011), pp. 2346-2349.

[43] H. Qu, S. Tong, K. Song, H. Ma, G. Bao, S. Pincus, W. Zhou, C. O'Connor. Controllable in situ synthesis of magnetite coated silica-core water-dispersible hybrid nanomaterials. Langmuir, 29 (2013), pp. 10573-10578.

[44] M. Blondeau, Y. Guyodo, F. Guyot, C. Gatel, N. Menguy, I. Chebbi, B. Haye, M. Durand-Dubief, E. Alphandery, R. Brayner, T. Coradin, Magnetic-field induced rotation of magnetosome chains in silicified magnetotactic bacteria. Sci. Rep., 8 (2018) 7699.

[45] T. Radu, C. Iacovita, D. Benea, R. Turcu. X-Ray Photoelectron Spectroscopic Characterization of Iron Oxide Nanoparticles. Appl. Surf. Sci., 405 (2017), pp. 337-343.

[46] R.M. Fratila, S. Rivera-Fernandez, J.M. de la Fuente. Shape matters: synthesis and biomedical applications of high aspect ratio magnetic nanomaterials. *Nanoscale*, 17 (2015), pp. 8233-8260.

[47] Z. Zhou, X. Zhu, D. Wu, Q. Chen, D. Huang, C. Sun, J. Xin, K. Ni, J. Gao, Anisotropic Shaped Iron Oxide Nanostructures: Controlled Synthesis and Proton Relaxation Shortening Effects. Chem. Mater., 27 (2015), pp. 3505-3515.

[48] G.F. Goya, T.S. Berquo, F.C. Fonseca, M.P. Morales. Static and dynamic magnetic properties of spherical magnetite nanoparticles. J. Appl. Phys., 94 (2003) 3520.

[49] H. Yang, L. Duan, Q. Li, Z. Tian, G. Li. Experimental and modeling investigation on the rheological behavior of collagen solution as a function of acetic acid concentration. J. Mech. Behav. Biomed. Mater., 77 (2018), pp. 125-134.

[50] C. Rodriguez-Rivero, L. Hilliou, E.M. Martin del Valle, M.A. Galan. Rheological characterization of commercial highly viscous alginate solutions in shear and extensional flows. Rheol. Acta, 53 (2014), pp. 559-570.